Novel approach in LC-MS/MS using MRM to generate a full profile of acyl-CoAs: discovery of acyl-dephospho-CoAs[S]

Qingling Li,* Shenghui Zhang,* Jessica M. Berthiaume,* Brigitte Simons,† and Guo-Fang Zhang[1,*]

Department of Nutrition,* Case Western Reserve University, Cleveland, OH 44106; and AB SCIEX,† Concord, Ontario L4K 4V8, Canada

Abstract **A metabolomic approach to selectively profile all acyl-CoAs was developed using a programmed multiple reaction monitoring (MRM) method in LC-MS/MS and was employed in the analysis of various rat organs. The programmed MRM method possessed 300 mass ion transitions with the mass difference of 507 between precursor ion (Q1) and product ion (Q3), and the precursor ion started from *m/z* 768 and progressively increased one mass unit at each step. Acyl-dephospho-CoAs resulting from the dephosphorylation of acyl-CoAs were identified by accurate MS and fragmentation. Acyl-dephospho-CoAs were also quantitatively scanned by the MRM method with the mass difference of 427 between Q1 and Q3 mass ions. Acyl-CoAs and dephospho-CoAs were assayed with limits of detection ranging from 2 to 133 nM. The accuracy of the method was demonstrated by assaying a range of concentrations of spiked acyl-CoAs with the results of 80–114%. The distribution of acyl-CoAs reflects the metabolic status of each organ. The physiological role of dephosphorylation of acyl-CoAs remains to be further characterized.** **The methodology described herein provides a novel strategy in metabolomic studies to quantitatively and qualitatively profile all potential acyl-CoAs and acyl-dephospho-CoAs.**—Li, Q., S. Zhang, J. M. Berthiaume, B. Simons, and G-F. Zhang. **Novel approach in LC-MS/MS using MRM to generate a full profile of acyl-CoAs: discovery of acyl-dephospho-CoAs.** ***J. Lipid Res.*** **2014.** 55: **592–602.**

Supplementary key words multiple reaction monitoring • liquid chromatography • mass spectrometry • rat organs

Acyl-CoAs are a class of important molecules that play essential roles in many physiological processes (1), such as fatty acid oxidation, lipid synthesis/remodeling, ketone body synthesis, xenobiotic metabolism, and signaling pathways. Classically, acyl-CoAs such as free CoA, acetyl-CoA, and malonyl-CoA are recognized as regulators of metabolic flux. The ratio of acetyl-CoA versus free CoA tightly regulates glycolysis and fatty acid oxidation. Malonyl-CoA attenuates fatty acid oxidation by inhibiting acyl-CoA transport into the mitochondrion for oxidation and is utilized in fatty acid synthesis when its concentration is elevated (2). Many proteins and genes are dynamically regulated by deacylation and acylation via various acyl-CoAs, such as acetyl-CoA, succinyl-CoA, palmitoyl-CoA, etc. (3). However, acyl-CoAs present in the cell are diverse and may involve molecules beyond fatty acids and their oxidized derivatives. The metabolism of xenobiotics can also lead to the formation of acyl-CoAs, as demonstrated in our previous work on the metabolism of 4-hydroxy acids from C_4 to C_{11} in perfused rat liver. The identification of these novel acyl-CoAs extends our understanding of the new catabolic pathways involved in the disposal of 4-hydroxy acids including drugs of abuse and lipid peroxidation products (4–8).

Acyl-CoAs are exclusive to the intracellular metabolites, and the profile of these biomolecules is indicative of the local metabolic status. Each organ has its specific physiological roles with different energetic demands, and therefore, would be expected to exhibit a unique acyl-CoA profile. The heart preferentially utilizes fatty acids to meet the ATP demand of mechanical contraction. Glucose and/or ketone bodies serve as the primary substrate of the brain for energy

This publication was made possible by the Case Western Reserve University/Cleveland Clinic CTSA (Clinical & Translational Science Awards) Grant UL1 RR024989 from the National Center for Research Resources to G-F.Z. and a component of the National Institutes of Health and National Institutes of Health Roadmap for Medical Research and AHA (American Heart Association) Award 12GRNT12050453 to G-F.Z. This work was supported, in whole or in part, by National Institutes of Health Roadmap Grants R33DK070291 and R01ES013925 (to H. Brunengraber, Nutrition Department, Case Western Reserve University). This work was also supported by a grant from the Cleveland Mt. Sinai Health Care Foundation.

Manuscript received 23 October 2013 and in revised form 10 December 2013.

Published, JLR Papers in Press, December 20, 2013
DOI 10.1194/jlr.D045112

Abbreviations: CE, collision energy; DP, declustering potential; LOD, limit of detection; LOQ, limit of quantitation; MRM, multiple reaction monitoring; RSD, relative standard deviation.

[1]To whom correspondence should be addressed.
e-mail: gxz35@case.edu

[S] The online version of this article (available at http://www.jlr.org) contains supplementary data in the form of six figures and one table.

metabolism. Both fatty acid oxidation and synthesis are highly active in the liver. The profile or fingerprint of the acyl-CoAs across these tissues should broadly reflect the metabolic preferences of these organs, but may also reveal additional roles of acyl-CoAs in cellular processes.

LC-MS/MS is the most sensitive method to analyze acyl-CoAs and various LC-MS or LC-MS/MS approaches have been reported [for a full review see (1)]. However, most methods only assay either short-, medium-, or long-chain acyl-CoAs (9–19). The best approach for acyl-CoA quantitation, so far, is to measure the target acyl-CoAs from short to long carbon chain length in a single method (20, 21). However, no methodology previously described allows quantitative profiling of acyl-CoAs for the purpose of targeted and untargeted acyl-CoA analysis. The challenges of profiling acyl-CoAs are as follows: *i*) Acyl-CoAs are a large category of metabolites that are present at a range of concentrations. *ii*) Acyl-CoAs vary widely in the polarity of the acyl moiety challenging LC method development. Alkaline mobile phases are mostly employed to improve peak shapes of long-chain acyl-CoAs (20, 22), however, high pH is deleterious for silica-based C18 columns and greatly diminishes the lifespan. *iii*) Not all acyl-CoAs have authentic compounds. *iv*) Multiple reaction mornitoring (MRM) or selected reaction monitoring is a sensitive MS/MS approach for targeted analysis, but limits broad profiling.

Although challenges of profiling acyl-CoAs exist, common fragmentation patterns of acyl-CoAs in LC-MS/MS were found by us and others (4, 6, 23, 24), and these common fragmentation patterns enable broad profiling. In this work, a novel MRM method was developed to quantitatively scan acyl-CoAs in different rat organs according to the characteristic fragmentation pattern of acyl-CoAs in MS/MS.

Dephospho-CoA and ATP are substrates of the last step of CoA synthesis catalyzed by dephospho-CoA kinase (25). Several acyl-dephospho-CoAs have been synthesized in vitro (26, 27), and valproyl-dephospho-CoA has been identified in isolated rat liver mitochondria from CoA trapping reagent (valproate), suggesting that both the phospho- and dephospho-CoA forms are biologically active (28). The absence of the 3′-phosphate group on the ribose moiety of acyl-dephospho-CoAs is the only difference compared with their corresponding acyl-CoAs. A similar MRM approach was also developed to quantitatively scan acyl-dephospho-CoAs in the rat organs.

The purpose of this work was to develop a MRM method to scan and quantitate acyl-CoAs and possibly acyl-dephospho-CoAs. With the developed method, we can quantitatively map all acyl-CoAs for both targeted and untargeted metabolomic studies.

METHODS

Materials

Acyl-CoAs from short to long carbon chain length (free CoA to C_{20}), dephospho-CoA, and heptadecanoyl-CoA (internal standard) were purchased from Sigma (St. Lois, MO). [2,2,3,3,3-$^2H_5$] propionyl-CoA and [2,2,3,3,4,4,5,5,5-$^2H_9$]pentanoyl-CoA were synthesized according to our previous work (4–6, 8). The aqueous stock solutions of acyl-CoAs were stored at −80°C.

Animal experiments

Adult male Sprague-Dawley rats (300–350 g) were fed ad libitum for 8–12 days with standard laboratory chow prior to the experiments. All experiments were performed in accordance with the Institutional Animal Care and Use Committee at Case Western Reserve University.

Fed rats were anesthetized with 5% isoflurane in an induction chamber, and maintained via facial mask at 2% during the surgical procedure. A median laparotomy was performed and a bolus of heparin (500 U/kg) was given via the inferior vena cava. Livers, hearts, kidneys, and brains were quickly dissected and frozen in liquid nitrogen until further analysis.

Preparations of acetyl-dephospho-CoA and butyryl-dephospho-CoA

To demonstrate that dephospho-CoA is a substrate of acetyl-CoA synthetase and to prepare authentic acyl-dephospho-CoA, the synthesis of acetyl-dephospho-CoA and butyryl-dephospho-CoA by acetyl-CoA synthetase was assayed (29). In microcentrifuge tubes, 10 mM sodium acetate or sodium butyrate, 10 mM $MgCl_2$, 50 mM KH_2PO_4, 10 mM ATP, and 0.7 mM dephospho-CoA were mixed into a final volume of 100 μl (pH 7.4). Acetyl-CoA synthetase (0.02 U) was added to the mixture to start the reaction at 37°C. The reaction was quenched by 500 μl acetonitrile after 1 h and enzyme was removed by centrifugation at 800 *g* for 15 min. The supernatant was dried and 100 μl Milli-Q water was added to redissolve the residue for LC-MS/MS analysis.

Sample preparation

Acyl-CoAs and acyl-dephospho-CoAs in various tissues were extracted using our previous methods (4–6, 8). Powdered tissues (250 mg), spiked with mixtures of internal standard {[2,2,3,3,3-$^2H_5$]propionyl-CoA (0.2 nmol), [2,2,3,3,4,4,5,5,5-$^2H_9$]pentanoyl-CoA (0.2 nmol), and heptadecanoyl-CoA (2 nmol)}, were homogenized for 1 min using a Polytron homogenizer after adding 4 ml of extraction buffer (methanol/water 1:1 containing 5% acetic acid). The supernatant was further purified by a 3 ml ion exchange cartridge packed with 300 mg of 2-(2-pyridyl)ethyl silica gel (Sigma). The cartridge was preactivated with 3 ml methanol, and then equilibrated with 3 ml of extraction buffer. Another 3 ml of extraction buffer was loaded to clean the sample after sample loading. The acyl-CoAs trapped on the silica gel cartridge were eluted by *i*) 3 ml of a 1:1 mixture of 50 mM ammonium formate (pH 6.3) and methanol, *ii*) 3 ml of a 1:3 mixture of 50 mM ammonium formate (pH 6.3) and methanol, and *iii*) 3 ml methanol. The combined effluent was dried with N_2 gas and stored at −80°C until LC-MS/MS analysis. The dried sample was used for all assays by TripleTOF 5600$^+$ and 4000 QTRAP mass spectrometers.

Acyl-dephospho-CoA identified by TripleTOF 5600$^+$

Dried samples were dissolved in 100 μl Milli-Q water and centrifuged for 15 min at 800 *g* to remove undissolved material. Two microliters of sample were injected into a 3C18-EP-120 column (0.5 × 50 mm, 3.0 μm, 120 Å) with the column oven temperature at 40°C. The LC-MS/MS system was a microLC (Ekspert™ microLC 200 system, AB SCIEX, Concord, ON, Canada) with a TripleTOF 5600$^+$ system (AB SCIEX). The temperature of the autosampler was set at 5°C and the flow rate was 40 μl/min. A gradient elution method was adopted as follows: 100% mobile

phase A (25 mM ammonium formate in 98% water and 2% acetonitrile, pH 8.2) was maintained from 0 to 0.3 min, mobile phase B (98% acetonitrile and 2% water, 5 mM ammonium formate) was increased linearly to 30% from 0.3 to 2.2 min and increased to 55% from 2.2 to 12 min, and finally increased to 100% within 1 min. The 100% mobile phase B was maintained for 4 min to clean the column, and then was returned to the initial condition in 0.5 min followed by column equilibration for 3 min. The total run time was 20.5 min. The TripleTOF 5600$^+$ mass spectrometer was set to electrospray ionization mode with an ion spray voltage of 5.5 kV, curtain gas of 25 psi, gas 1 of 60 psi, gas 2 of 30 psi, and an interface heater temperature of 350°C. The *m/z* of the TOF mass scan was from 300 to 1,250 with an accumulation time of 0.6 s, a declustering potential (DP) of 60 V, and a minimum collision energy (CE) voltage of 5 V. The data-independent workflow mode (SWATH acquisition) was set up to acquire full scan MS/MS data of precursor ions (*m/z* from 100 to 1,250) in 60 amu increments. The DP and CE for SWATH acquisition were 60 and 50 V, respectively.

Acyl-CoA and acyl-dephospho-CoA profiled by LC-MS/MS

After dissolving the acyl-CoAs in 100 μl of mobile phase A (2% acetonitrile in 100 mM ammonium formate, pH 5.0), a 40 μl sample was injected on an Agilent ZORBAX 300SB-C8 column (100 × 2.1 mm, 3.5 μm) protected by a guard column (ZORBAX) (5 μm, 12.5 × 2.1 mm) in a Dionex-UltiMate 3000 LC system. The temperatures of column oven and autosampler were set at 42 and 5°C, respectively. The LC method was developed at 0.2 ml/minute, and *i*) started with 100% mobile phase A and 0% mobile phase B (98% acetonitrile in 5 mM ammonium formate, pH 6.3) for the initial 2 min, *ii*) mobile phase B was increased to 60% within 8 min, *iii*) then mobile phase B was further increased to 90% in 1 min and maintained at 90% for 19 min, and *iv*) the gradient was finally returned to the initial condition within 1 min and the column was reequilibrated with the initial condition for 10 min before the next injection.

The liquid chromatograph was coupled to a 4000 QTRAP mass spectrometer (Applied Biosystems, Foster City, CA) operated under positive ionization mode with the following source settings: turbo-ion-spray source at 500°C under N_2 nebulization at 65 psi, N_2 heater gas at 55 psi, curtain gas at 30 psi, collision-activated dissociation gas pressure was held at high, turbo ion-spray voltage at 5,500 V, DP at 90 V, entrance potential at 10 V, CE at 50 V, and collision cell exit potential at 10 V. There was no detectable acyl-CoA located at *m/z* between 769 and 809 (*m/z* from free CoA to acetyl-CoA), thus we skipped precursor ion (Q1) from 770 to 807. This allowed us to set up the MRM method with the Q1 ions from 768 to 1,100, and their corresponding product ion (Q3) ions as the subtraction of the Q1 ions by 507. Multiple fragments of some acyl-CoAs, such as methylmalonyl-CoA, were added to the MRM transitions to make sure the separation of isobaric acyl-CoAs. In a separate acyl-dephospho-CoA MRM method, the Q1 ions started from 688 to 988, with the Q3 ions as the subtraction of their corresponding Q1 ions by 427. Analyst software (version 1.4.2; Applied Biology) was used for data registration.

Method validation

The method was validated using commercially available acyl-CoAs and dephospho-CoAs in terms of assay linearity, sensitivity, precision, and accuracy. Sensitivity of the assays was determined in terms of limits of detection (LODs) and limits of quantitation (LOQs), which were evaluated by series dilution of standards. LODs and LOQs are determined as the concentrations which yield the peak with 3 S/N (signal/noise) and 10 S/N, respectively. Accuracy was determined by a process of spiking of analytes into diluted rat heart homogenates (n = 4–5) and evaluating by LC-MS/MS analysis. The diluted rat heart homogenates were prepared by continuous dilution with extraction buffer until no acyl-CoAs were detected.

Statistical analyses

The heat map of average concentrations of acyl-CoAs and acyl-dephospho-CoAs was processed by PermutMatrix (Montpellier Laboratory, France) (30). The significant *P* value for the correlation is set at <0.05. Statistical differences were tested using a paired *t*-test (Graph Pad Prism software, version 3).

RESULTS

All acyl-CoAs were determined to have the following common fragmentation patterns in positive electrospray ionization-MS/MS (**Fig. 1**): *i*) fragment *m/z* 428 that represents the CoA moiety, and *ii*) a neutral loss of 507 which is the 3′-phosphonucleoside diphosphate fragment. The fragment of acyl-CoAs from the neutral loss of 507 was the most abundant fragment, and this fragment was used for acyl-CoA MRM assays. DP and CE are essential parameters in MS/MS and are very similar for all acyl-CoAs from short- to long-chain length. Hence, a programmed MRM method was designed to scan all acyl-CoAs. The precursor ion in Q1 started from 768 (free CoA, the smallest acyl-CoAs), and progressively increased to 1,100 (*m/z* from 770 to 807 was skipped in this work because there are no known acyl-CoAs from animal tissues located in this mass range, but it can be added if it is needed) by one mass unit increase at each step. The corresponding product ion in Q3 was the Q1 minus 507 and started from 261 (free CoA) to 593. About 300 ion transitions were determined to sufficiently cover the range of known acyl-CoAs, but can be extended to a higher mass range using a second method.

In addition to classically recognized acyl-CoAs, a subset of acyl-CoA analogs was identified in TripleTOF 5600$^+$ that attracted our attention and warranted further investigation. The metabolites of interest had the following characteristics: *i*) a fragment from the neutral loss of 427 (acyl-CoAs have the similar fragment, but from a neutral loss of 507); *ii*) a common fragment at *m/z* 348 (acyl-CoAs have a common fragment at *m/z* 428, 80 amu higher than *m/z* 348); *iii*) precursor ions of metabolites with 80 amu less than the corresponding acyl-CoAs; and *iv*) a longer retention time compared with the corresponding acyl-CoAs. From these observations, we concluded that these metabolites were acyl-dephospho-CoAs. The representative LC-TripleTOF 5600$^+$ data is shown in **Fig. 2**.

The detailed fragmentation patterns of acyl-dephospho-CoAs are outlined in Fig. 1. Acyl-dephospho-CoAs displayed the same fragmentation profile as acyl-CoAs assayed by electrospray ionization-MS/MS. The absence of a phosphate group at the 3′-ribose moiety of acyl-dephospho-CoAs leads to a neutral loss of 427 rather than 507 for acyl-CoAs, and the other common fragment (5′-phosphoadenosine) of acyl-dephospho-CoAs becomes *m/z* 348 corresponding to *m/z* 428 for acyl-CoA.

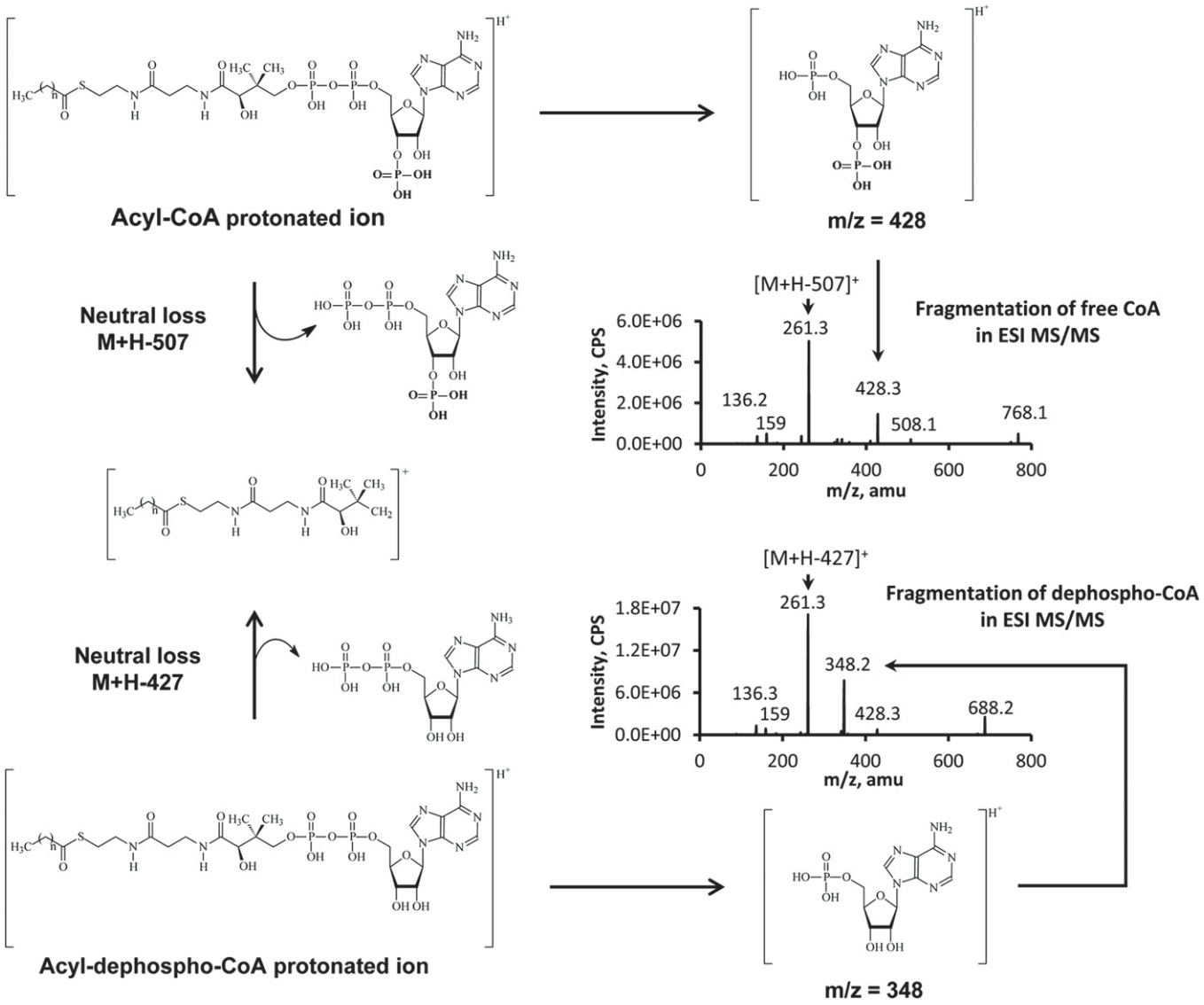

Fig. 1. The fragmentation of acyl-CoAs and acyl-dephospho-CoAs in MS/MS. The 3′-phospho group is the only difference between acyl-CoAs and acyl-dephospho-CoAs, and this difference is reflected by the mass difference of 80 in neutral loss and fragment as well.

To further verify the identity of these CoA analogs, dephospho-CoA standard and two other acyl-dephospho-CoAs (acetyl-dephospho-CoA and butyryl-dephospho-CoA) were synthesized in vitro from dephospho-CoA by acetyl-CoA synthetase. The resulting data confirmed the identities of acyl-dephospho-CoAs (supplementary Fig. I).

HPLC separation of free CoA and all acyl-CoAs ranging from free CoA to C_{22} was investigated on several reversed phase columns, mobile phases, and gradient elution profiles in order to define optimal assay conditions. Long-chain acyl-CoAs have very broadened peak shapes, if all acyl-CoAs including short-chain acyl-CoAs need to be included in one method. A high percentage of organic solvent during the initial conditions would be expected to improve the broadening peaks of long-chain acyl-CoAs. However, some isobaric acyl-CoAs (short-chain length) would then coelute under these conditions, such as malonyl-CoA, 3-hydroxybutyryl-CoA, methylmalonyl-CoA, and succinyl-CoA. A C_8 reversed phase column was found to be able to reasonably separate all acyl-CoAs from short- to long-chain length. Increasing ammonium formate in mobile phase A greatly improved peak tailing (though the maximal concentration achieved was solubility-limited); the final concentration of ammonium formate employed was 100 mM in mobile phase A and 5 mM in mobile phase B. The pH of mobile phase A found to be optimal at 5.0, used a column with oven temperature at 42°C.

The incidence of peak overlap was also addressed, as methylmalonyl-CoA is a structural isomer of succinyl-CoA. Succinyl-CoA is present in much higher concentrations than methylmalonyl-CoA, so a methylmalonyl-CoA-specific fragment at *m/z* 317 was used as a means to ensure selective quantitation. Under the optimized LC conditions, acyl-dephospho-CoAs were well-separated with retention times lagging 1–2 min behind the corresponding acyl-CoAs due to the loss of a polar phosphate group.

The calibration curve, linearity, and sensitivity (LODs and LOQs) of acyl-CoAs and dephospho-CoAs are shown

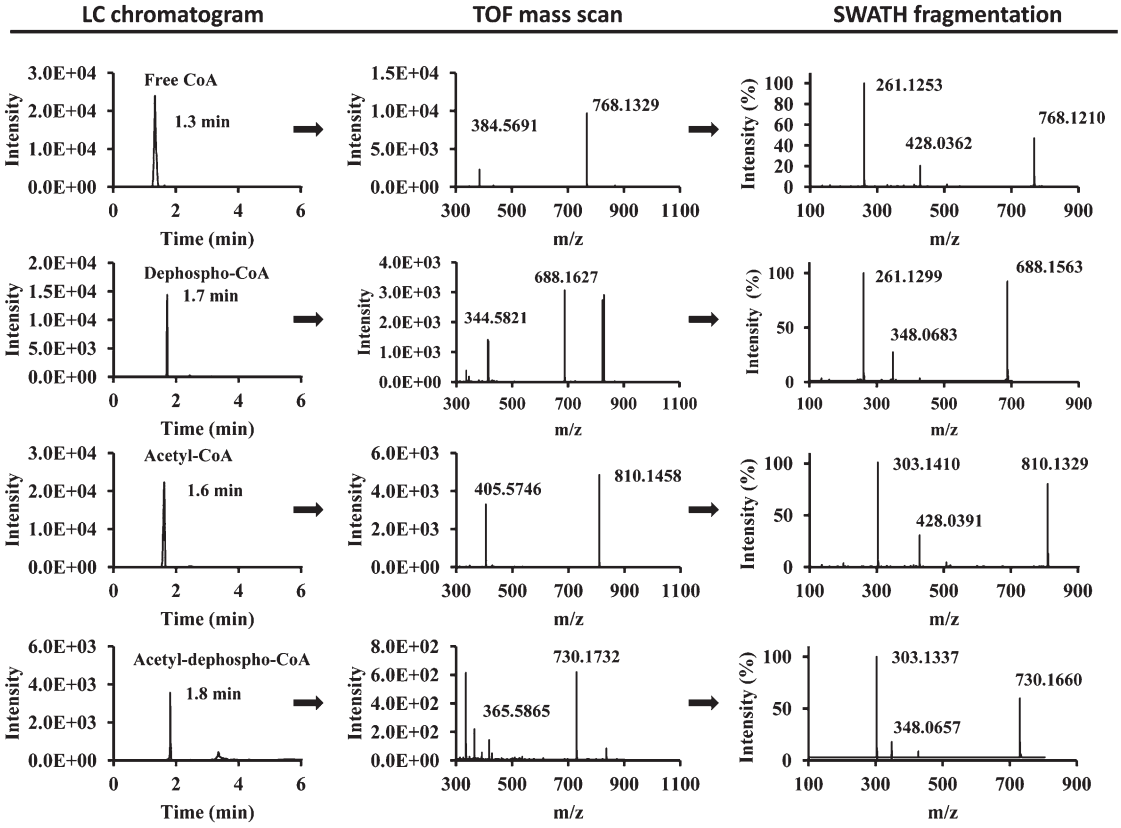

Fig. 2. Extracted data of free CoA, dephospho-CoA, acetyl-CoA, and acetyl-dephospho-CoA in the heart analyzed by MicroLC-TripleTOF 5600^{+}. Extracted LC chromatograms, TOF mass scans, and SWATH fragmentation patterns for free CoA (first row), dephospho-CoA (second row), acetyl-CoA (third row), and acetyl-dephospho-CoA (fourth row). The details of the experiments are described in the Methods section.

in **Table 1**. All acyl-CoAs and dephospho-CoAs show good linear signal response across the concentration ranges of the acyl-CoAs assessed. The programed MRM method is very sensitive to short- and medium-chain length acyl-CoAs and dephospho-CoAs. The lower sensitivity to long-chain acyl-CoAs is likely due to the slight peak broadening and/or low ionization yield. All the measured standard acyl-CoAs had some noticeable degradation over the time at 4°C in the autosampler. However, normalized to the internal standard, the relative standard deviations (RSDs) of continuous measurements over 27 h for acyl-CoAs at 4°C in the autosampler were from 11.1 to 23.3%.

Methodological accuracy was evaluated by measuring the known amount of acyl-CoAs spiked into diluted heart extracts. Diluted heart extracts (which possessed no endogenous acyl-CoAs or acyl-dephospho-CoAs) were spiked with different quantities of acyl-CoAs and dephospho-CoAs (very low, low, medium, and high concentrations; the amounts of each compound at different quantities are listed in supplementary Table I). The choice of spiked quantities was based on the concentrations of acyl-CoAs found in real samples. Spiked samples were analyzed and data are presented in **Table 2**. The results in Table 2 indicate that the developed MRM method possesses high accuracy for both acyl- and dephospho-CoAs. The RSDs of assays at all concentrations of acyl-CoAs were below 15%, which shows the high precision of the method.

TABLE 1. LODs, LOQs, and calibration curves of LC-MS/MS quantitation method for acyl-CoAs

	Linearity	R^2	LOD (nM)	LOQ (nM)
Free CoA	y = 0.4x − 0.009	0.9993	20	63
Acetyl-CoA	y = 1.4x + 0.1	0.9919	6	13
Propionyl-CoA	y = 3.5x − 0.1	0.9957	10	25
Malonyl-CoA	y = 0.1x + 0.0005	0.9958	20	50
Succinyl-CoA	y = 0.6x − 0.1	0.9954	3	5
Methylmalonyl-CoA	y = 0.9x + 0.02	0.9940	60	200
Octanoyl-CoA	y = 1.6x + 0.1	0.9962	20	60
Palmitoyl-CoA	y = 1.5x + 0.2	0.9998	71	250
C18:2-CoA	y = 0.6x + 0.1	0.9998	133	333
C20:4-CoA	y = 0.8x + 0.1	0.9993	100	333
Dephospho-CoA	y = 1.9x + 0.1	0.9944	2	7

TABLE 2. Accuracy of LC-MS/MS method by comparing the measured acyl-CoAs to the spiked amounts at different concentrations

	Very Low	Low	Medium	High
Free CoA	98 ± 10	104 ± 6	81 ± 10	108 ± 7
Acetyl-CoA	100 ± 14	105 ± 12	98 ± 12	97 ± 11
Propionyl-CoA	93 ± 12	95 ± 9	100 ± 3	93 ± 6
Succinyl-CoA	108 ± 8	114 ± 6	91 ± 7	107 ± 3
Malonyl-CoA	83 ± 10	81 ± 6	80 ± 4	91 ± 12
Methylmalonyl-CoA	84 ± 9	87 ± 6	95 ± 7	96 ± 9
Octanoyl-CoA	91 ± 10	97 ± 8	105 ± 10	101 ± 10
Palmitoyl-CoA	99 ± 9	89 ± 11	97 ± 11	82 ± 11
C18:2-CoA	92 ± 7	91 ± 14	94 ± 13	96 ± 5
C20:4-CoA	93 ± 10	99 ± 4	98 ± 10	111 ± 4
Dephospho-CoA	97 ± 12	81 ± 5	91 ± 14	105 ± 13

Data in the table are expressed as: assayed concentration/spiked concentration × 100% ± standard deviation.

Acyl-CoAs possess structural diversity to include saturated, unsaturated, hydroxylated, and dicarboxyl functional groups in the acyl chain. The concentrations of acyl-CoAs range from trace amounts to relatively high abundance depending on the specific acyl-CoA and the tissue type of interest. In general, liver was determined to contain the greatest quantity of total acyl-CoAs (**Fig. 3**), and brain the lowest (Fig. 3).

To clearly visualize and compare the fingerprint of acyl-CoAs across tissue types, we mapped four categories of acyl-CoAs in rat heart, kidney, liver, and brain by constructing heat maps. The data in the heat maps are from the average concentration (nmol/g wet weight) of acyl-CoAs in each organ assayed. The RSDs of all measured acyl-CoAs in various organs is not shown in the heat maps, but was <20% for all assays (n = 3–4). The concentrations of acyl-CoAs for which direct standards could not be obtained were calculated based on the calibration curve of a suitable standard acyl-CoA which was in close proximity on the chromatogram.

Figure 4A shows the distribution of saturated acyl-CoAs (from free CoA to C_{18}-CoA, including methylmalonyl-CoA and HMG-CoA) in rat hearts, kidneys, livers, and brains. Not all saturated acyl-CoAs have the standards. Therefore, identification of some saturated acyl-CoAs was based on the measured mass, fragmentation pattern, and chromatographic properties (extracted chromatograms of saturated acyl-CoAs from various tissues are shown in supplementary Fig. II). The highest amounts of free CoA and acetyl-CoA are in the kidney and liver (~30 nmol/g wet weight). Interestingly, the kidney has relatively higher amounts of other short- and medium-chain saturated acyl-CoAs (C_3 to C_{10}) compared with other organs tested. Odd carbon number acyl-CoAs, such as heptanoyl-CoA and pentanoyl-CoA, are uncommon acyl-CoAs. Surprisingly, they were found to be present in relatively high amounts in the kidney. The highest amount of propionyl-CoA was also found in the kidney. Saturated acyl-CoAs with a carbon chain length >C_{10} were in the highest abundance in the heart. The brain

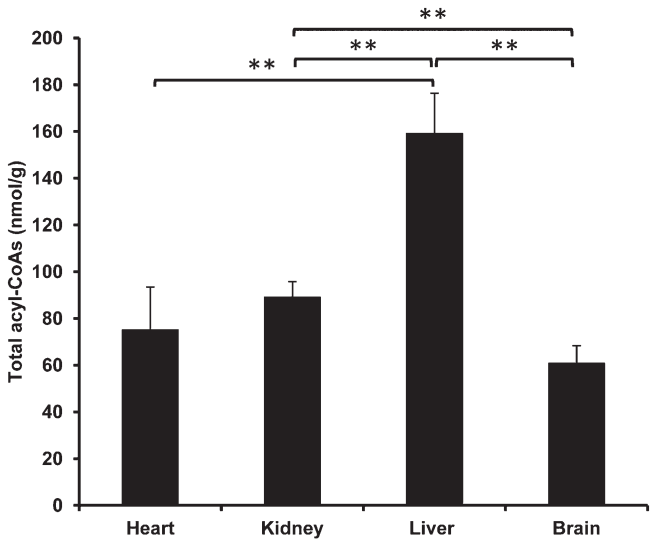

Fig. 3. Total acyl-CoAs (nmol/g wet weight) found in rat heart, kidney, liver, and brain. The total amount of acyl-CoAs is the sum of all measured acyl-CoAs by LC-MS/MS. The significant difference of total acyl-CoAs between each two organs is indicated by ** ($P < 0.05$).

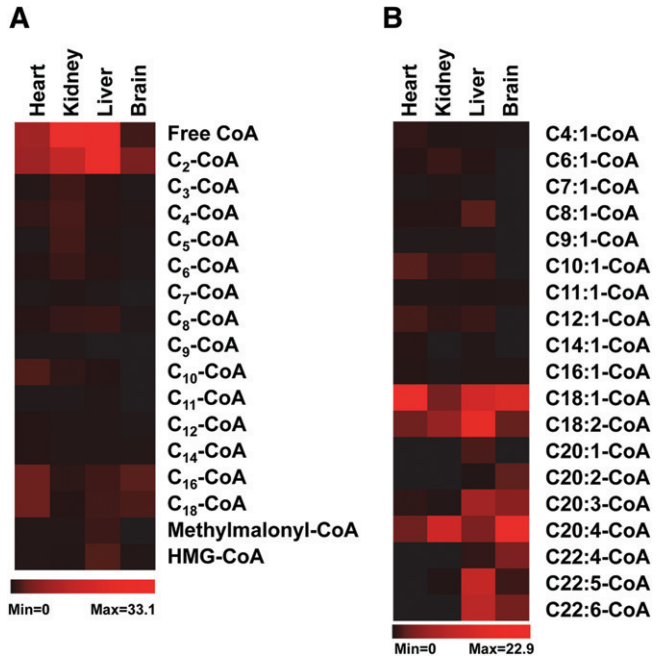

Fig. 4. The distributions of saturated acyl-CoAs and unsaturated acyl-CoAs in rat heart, kidney, liver, and brain (n = 3–4). Red and black colors represent high and low concentrations, respectively, of measured acyl-CoAs. A: Saturated acyl-CoA, concentration range is from 0 to 33.1 nmol/g. B: Unsaturated acyl-CoA, concentration range is from 0 to 22.9 nmol/g.

also had relatively high concentrations of C_{16}-CoA and C_{18}-CoA. Methylmalonyl-CoA and HMG-CoA were predominantly found in the liver, whereas other organs possessed 5- to 10-fold lower quantities of each.

The distribution of unsaturated acyl-CoAs in the rat organs tested is shown in Fig. 4B. The chromatograms for these unsaturated acyl-CoAs from various tissues can be found in supplementary Figs. III-1 and III-2. Unsaturated acyl-CoAs eluted out slightly earlier than their corresponding saturated acyl-CoAs (supplementary Figs. II, III-1). Unsaturated acyl-CoAs clustered into two groups according to their concentrations found in organs. The first group is the long-chain unsaturated acyl-CoAs, such as C18:1-, C18:2-, and C20:4-CoA, that are present at high concentrations in all organs; other long-chain unsaturated acyl-CoAs, like C20:1-, C20:2-, C20:3-, C22:4-, C22:5-, and C22:6-CoA, mostly locate in the liver and brain. The second group of unsaturated acyl-CoAs with a carbon chain length $<C_{16}$ are below 2 nmol/g wet weight in all four organs, and nearly undetectable in the brain. The heart and liver have relatively high levels of unsaturated acyl-CoAs (C_4–C_{16}).

3-Hydroxyacyl-CoAs are β oxidation intermediates of fatty acids. 3-Hydroxyacyl-CoAs from various tissues were identified according to standard and their retention time (supplementary Fig. IV). The hydroxyl group leads 3-hydroxyacyl-CoAs to be more polar compared with their corresponding acyl-CoAs and mono-unsaturated acyl-CoAs, and this can be demonstrated by their retention times (supplementary Fig. IV). C_n-3-hydroxyacyl-CoA has the same mass and mass transition as C_{n-1}-dicarboxyl-CoA, this leads to more than one peak in an extracted chromatogram (supplementary Fig. IV), and it is the same for dicarboxyl-CoAs (see the section below and supplementary Fig. V).The concentrations of 3-hydroxyacyl-CoAs in tissues are mapped in **Fig. 5A**. Relatively high levels of 3-hydroxyacyl-CoAs, particularly those with a carbon chain length >10, are found in the heart. Only trace amounts of 3-hydroxyacyl-CoAs are found in brain samples.

The well-known and small dicarboxyl-CoAs are malonyl-CoA (C_3), succinyl-CoA (C_4), and methylmalonyl-CoA (C_4). As expected, malonyl-CoA, succinyl-CoA, and methylmalonyl-CoA were present in all organs, except for trace amounts of malonyl-CoA (20- to 30-fold lower) and undetectable

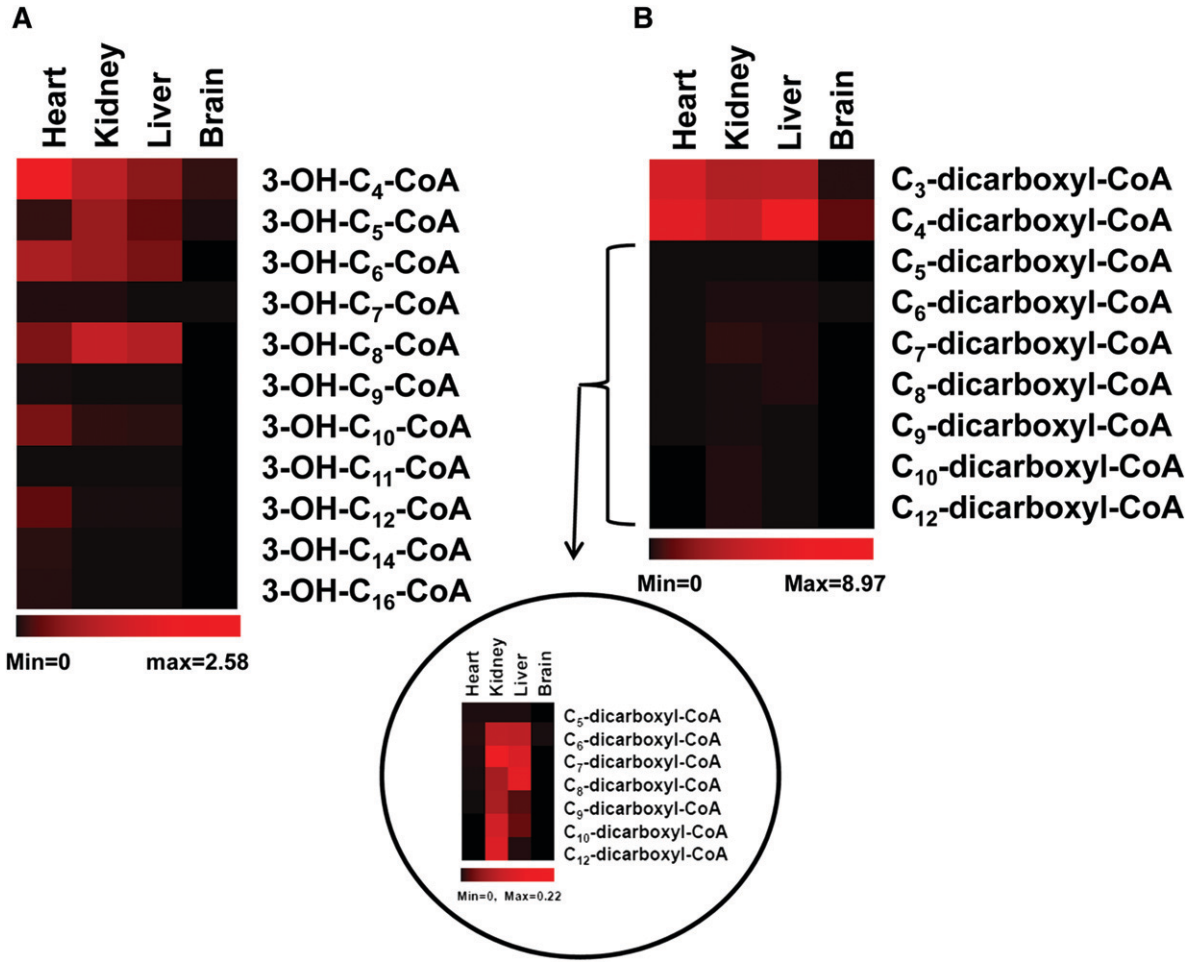

Fig. 5. The distributions of 3-hydroxyacyl-CoAs and dicarboxyl-acyl-CoAs in rat heart, kidney, liver, and brain. Red and black colors represent high and low concentrations, respectively, of measured acyl-CoAs. The concentration data of acyl-CoAs is the average of 3–4 rats. A: 3-Hydroxyacyl-CoAs, concentration range is from 0 to 2.58 nmol/g. B: Dicarboxyl-acyl-CoAs, concentration range is from 0 to 8.97 nmol/g. The distribution of dicarboxyl-acyl-CoAs from C_5 to C_{12} is zoomed in the circled insert, concentration range of the insert is from 0 to 0.22 nmol/g.

methylmalonyl-CoA in the brain (Figs. 4A, 5B). Surprisingly, both the kidney and liver had dicarboxyl-CoAs (C_6–C_{12}), but they were not found in the heart or brain. In addition, the kidney had relatively higher levels of these medium-chain dicarboxyl-CoAs compared with the liver. The extracted chromatograms of the measured dicarboxyl-CoAs from various tissues are shown in supplementary Fig. V. The relatively short retention times of dicarboxyl-CoAs compared with their corresponding acyl-CoAs, monounsaturated acyl-CoAs, and 3-hydroxyacyl-CoAs are due to the polar carboxylic group.

Figure 6 shows the acyl-CoA compositions of rat organs according to structural characteristics (i.e., saturated acyl-CoA, unsaturated acyl-CoA, hydroxyacyl-CoA, and dicarboxyl-acyl-CoA). Noteworthy is that succinyl-CoA, methylmalonyl-CoA, and malonyl-CoA are related to the citric acid cycle, amino acid metabolism, and fatty acid synthesis, and they are different from other dicarboxyl-acyl-CoAs resulting from omega oxidation. Therefore, succinyl-CoA, methylmalonyl-CoA, and malonyl-CoA were included in the saturated acyl-CoA category. In this way, rat heart has 51% saturated acyl-CoAs, 43% unsaturated acyl-CoAs, 6% hydroxyl-acyl-CoAs, and a small amount of dicarboxyl-acyl-CoAs (<0.1%); rat kidney has 70% saturated acyl-CoAs, 25% unsaturated acyl-CoAs, 4% hydroxyl-acyl-CoAs, and 1% dicarboxyl-CoAs; and rat liver has 54% saturated acyl-CoAs, 44% unsaturated acyl-CoAs, 1% hydroxyl-acyl-CoAs, and less than 1% dicarboxyl-CoAs. The brain is mainly comprised of saturated acyl-CoAs (22%) and unsaturated acyl-CoAs (77%). Minimum quantities of hydroxyl-acyl-CoAs (<1%) are found in the brain and dicarboxyl-acyl-CoAs are minimal (<0.1%).

The acyl-dephospho-CoAs in four rat organs are listed in **Table 3**. The highest levels of acyl-dephospho-CoAs were found in the kidney. Only dephospho-CoA and acetyl-dephospho-CoA were detected in all four organs. The ratios of dephospho-CoA/free CoA and acetyl-dephospho-CoA/acetyl-CoA were calculated and are shown in **Fig. 7**. Both the brain and kidney had higher dephosphorylation ratios compared with the heart and liver.

DISCUSSION

MS is the most sensitive method for metabolomic studies. The development of MRM improves the analytical sensitivity of this approach by allowing the selection of both precursor and product ions. However, MRM is most commonly applied in the quantitation of a targeted compound. In the current study, the development of a MRM method based on the fragmentation pattern was successfully used to quantitatively profile both known and unknown acyl-CoAs and acyl-dephospho-CoAs in various rat organs with high sensitivity and accuracy. In total, 67 acyl-CoAs and acyl-dephospho-CoAs were characterized in the organs tested, and many acyl-CoAs and acyl-dephospho-CoAs lacking compound authentication were identified by their mass, fragmentation (loss of 507 for acyl-CoAs or 427 for acyl-dephospho-CoAs), and chromatographic retention time. Our results are in agreement with previously reported values (24), suggesting the untargeted approach by MRM accurately reflects quantities across the range of carbon chain lengths of physiologically relevant acyl-CoAs. Furthermore, the relative profiles of acyl-CoAs and acyl-dephospho-CoAs are in-line with the well-established metabolic function and demand in the respective tissues assayed. Liver tissue has high metabolic activity related to pathways, such as fatty acid oxidation, lipid synthesis, glucose oxidation, gluconeogenesis, and xenobiotic detoxification, which is in-line with the finding that liver contains the highest quantity of total acyl-CoAs (Fig. 3). Although the unsaturated acyl-CoAs and hydroxyacyl-CoAs found in the present work cannot exclude other possible isomers,

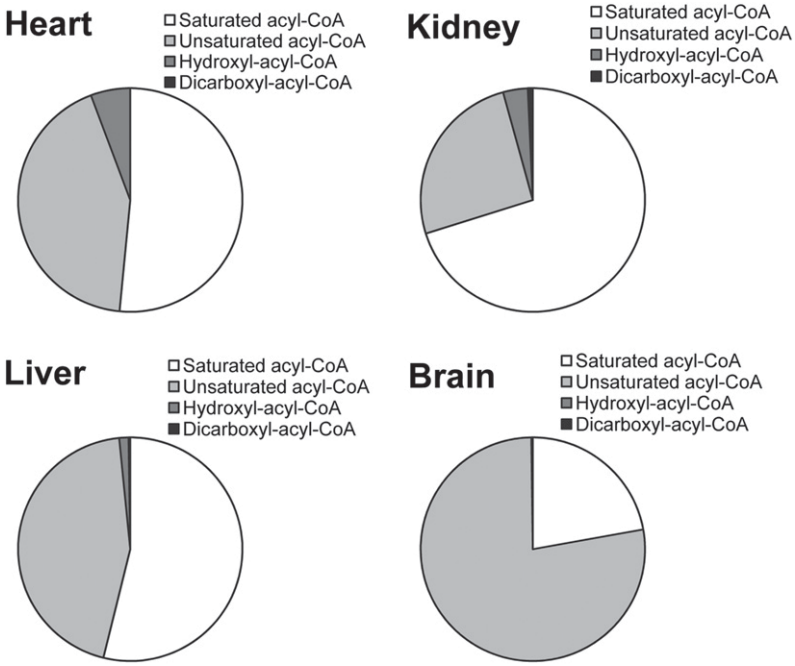

Fig. 6. The composition of acyl-CoA in each rat organ. The sum of each category of acyl-CoAs composes the pie figure of each organ. Methyl-malonyl-CoA and succinyl-CoA were calculated as saturated acyl-CoAs.

TABLE 3. Acyl-dephospho-CoA found in rat organs

Acyl-dephospho-CoAs	Heart (nmol/g)	Kidney (nmol/g)	Liver (nmol/g)	Brain (nmol/g)
Dephospho-CoA	0.01 ± 0.01	4.3 ± 0.8	0.5 ± 0.03	0.1 ± 0.01
C_2-dephospho-CoA	0.2 ± 0.003	3.2 ± 0.09	1.0 ± 0.02	1.0 ± 0.09
C_3-dephospho-CoA	ND	1.4 ± 0.3	0.04 ± 0.01	0.02 ± 0.01
C_4-dephospho-CoA	0.02 ± 0.007	0.5 ± 0.02	0.02 ± 0.008	0.01 ± 0.01
C_5-dephospho-CoA	ND	0.6 ± 0.05	0.004 ± 0.005	ND
C_6-dephospho-CoA	ND	0.3 ± 0.07	0.03 ± 0.003	ND
C_7-dephospho-CoA	ND	0.04 ± 0.01	ND	ND
C_8-dephospho-CoA	0.01 ± 0.002	0.4 ± 0.02	0.04 ± 0.0009	ND
Succinyl-dephospho-CoA	0.005 ± 0.002	0.09 ± 0.02	0.04 ± 0.009	ND
Malonyl-dephospho-CoA	0.003 ± 0.002	0.1 ± 0.03	0.01 ± 0.004	ND

n = 3∼4. ND, not detected.

enoyl-CoAs and 3-hydroxyacyl-CoAs are major physiological metabolites. And with the sample purification, neutral loss scan, and retention time, this method possesses good confidence of acyl-CoA and acyl-dephospho-CoA identification. However, interferences (non-acyl-CoAs or nonacyl-dephospho-CoAs) with similar characteristics still cannot be excluded. Therefore, caution should be taken in identifying acyl-CoAs with this method in certain circumstances, such as acyl-CoA metabolites from xenobiotics or drugs. In such cases, further characterization is needed to confirm their identities, such as using fragment ion scans, high resolution MS, isotope labeling, or authentic compounds.

The heart is a high energy demand organ where fatty acids serve as the preferred energy fuel for ATP production. This metabolic phenotype is reflected in our mapped data: *i*) several saturated acyl-CoAs (C_{10}-, C_{12}-, C_{14}-, and C_{18}-CoAs) are the highest in heart; *ii*) the corresponding unsaturated acyl-CoAs and 3-hydroxyacyl-CoAs, i.e., C_{10}-, C_{12}-, C_{14}-, and C_{18}-CoAs, are also relatively high in the heart. Saturated acyl-CoAs, enoyl-CoAs, and 3-hydroxyacyl-CoAs are β oxidation intermediates of fatty acids, the high amounts of these acyl-CoAs reflect the high activity of fatty acid oxidation in the heart.

Interestingly, high amounts of short- and medium-chain saturated acyl-CoAs (C_3–C_{10}) were present in the kidney. This is possibly due to reabsorption of acyl-carnitines by the kidney and further metabolism for energy production in the kidney. Odd chain saturated acyl-CoAs (heptanoyl-CoA and pentanoyl-CoA) were also found in particularly high amounts in kidney tissue and do not appear to come from the β oxidation of long-chain fatty acids with odd carbon numbers because longer chain acyl-CoAs (C > 7) with odd carbon numbers were not detected. We also observed that the kidney contained the highest amount of propionyl-CoA, a downstream metabolite of both pentanoyl-CoA and heptanoyl-CoA. Propionyl-CoA is an anaplerotic substrate that enters the citric acid cycle via carboxylation and isomerization to methylmalonyl-CoA and succinyl-CoA, respectively (31, 32). However, methylmalonyl-CoA and succinyl-CoA are not equivalently high in the kidney; 10-fold less, and one-half that of liver, respectively. This mismatched concentration of methylmalonyl-CoA or succinyl-CoA may be linked to the lower amount of ATP in the kidney, as ATP is involved in the carboxylation of propionyl-CoA to methylmalonyl-CoA.

The brain prefers glucose or ketone bodies as energy fuel and β oxidation of fatty acids is a minor contribution. This was reflected in the acyl-CoA fingerprint generated with our methodological approach. The largest portion of acyl-CoAs is long-chain saturated and unsaturated acyl-CoAs (C_{16} or above), representing ∼86% of total acyl-CoAs in the rat brain. Long-chain unsaturated fatty acids, such as oleic acid and arachidonic acid, are largely used for phospholipid synthesis and must be activated to acyl-CoAs before being used in the synthesis of phospholipids for incorporation into membranes (33, 34). The high abundance long-chain acyl-CoAs and diminutive amounts of other acyl-CoAs strongly indicate low β oxidation and high lipid synthesis, particularly phospholipids, in the brain. Beta oxidation intermediates, such as enoyl-CoAs and 3-hydroxyacyl-CoAs, were negligible in the brain.

Dicarboxyl-CoAs, except for malonyl-CoA, succinyl-CoA, and methylmalonyl-CoA, are metabolites of omega oxidation of medium-chain or long-chain fatty acids. Omega oxidation of fatty acids is initiated from omega hydroxylation by P450 enzymes at the terminal (omega) carbon of the fatty acid (35). We have recently observed that the kidney and liver have high omega hydroxylation activity,

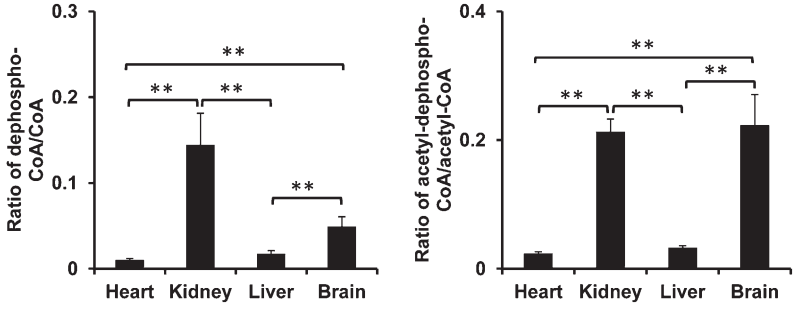

Fig. 7. The ratios of dephospho-CoA/free CoA and acetyl-dephospho-CoA/acetyl-CoA in rat heart, kidney, liver, and brain. Left panel: the ratio of dephospho-CoA/free CoA found in four organs. Right panel: the ratio of acetyl-dephospho-CoA/acetyl-CoA found in four organs. The significant difference of ratios between each two organs is indicated by ** ($P < 0.05$).

whereas the heart and brain are very low (Q. Li et al., unpublished observations). This is consistent with the relatively high quantities of short- and medium-chain dicarboxyl-acyl-CoAs in the liver and kidney and the negligible amounts in the heart and brain in this study.

Summarized from the acyl-CoA fingerprint in four organs as shown in the pie figure (Fig. 6), enoyl-CoAs (from C_4–C_{16}) and hydroxyl-CoAs in the heart indicate high fatty acid oxidation activity in the heart. Long-chain unsaturated acyl-CoAs in the brain suggest high lipid synthesis turnover in the brain (36). Undetectable amounts of hydroxyacyl-CoAs and dicarboxyl-CoAs in the brain indicate the low fatty acid oxidation and omega hydroxylation activities in the brain. The kidney and liver contain the most acyl-CoAs. The small portion of dicarboxyl-CoAs in the liver and kidney suggests the alternative fatty acid oxidation present in both organs. Dephosphorylation of acyl-CoAs seems to be a ubiquitous phenomenon. The physiological role of acyl-dephospho-CoAs needs to be further investigated. However, they were found to be related with ATP status. Both the brain and kidney were found to possess a lower concentration of ATP compared with the heart and liver (data not shown). ATP hydrolysis in the brain could occur during the sampling process because ATP dramatically drops within minutes in the ischemic brain (37).

The developed MRM method in this study provides a fundamental MRM strategy for other metabolomic studies focusing on a particular class of metabolites. This approach allowed us to produce an accurate profile of a wide range of cellular acyl-CoAs including characterization of a novel class of CoAs, the acyl-dephospho-CoAs, in various tissues. This MRM strategy can be extended to any category of analytes that have the same neutral loss or the same fragment.

REFERENCES

1. Haynes, C. A. 2011. Analysis of mammalian fatty acyl-coenzyme A species by mass spectrometry and tandem mass spectrometry. *Biochim. Biophys. Acta.* **1811:** 663–668.
2. Ussher, J. R., and G. D. Lopaschuk. 2008. The malonyl CoA axis as a potential target for treating ischaemic heart disease. *Cardiovasc. Res.* **79:** 259–268.
3. Newman, J. C., W. He, and E. Verdin. 2012. Mitochondrial protein acylation and intermediary metabolism: regulation by sirtuins and implications for metabolic disease. *J. Biol. Chem.* **287:** 42436–42443.
4. Harris, S. R., G. F. Zhang, S. Sadhukhan, A. M. Murphy, K. A. Tomcik, E. J. Vazquez, V. E. Anderson, G. P. Tochtrop, and H. Brunengraber. 2011. Metabolism of levulinate in perfused rat livers and live rats: conversion to the drug of abuse 4-hydroxypentanoate. *J. Biol. Chem.* **286:** 5895–5904.
5. Harris, S. R., G. F. Zhang, S. Sadhukhan, H. Wang, C. Shi, M. A. Puchowicz, V. E. Anderson, R. G. Salomon, G. P. Tochtrop, and H. Brunengraber. 2013. Metabolomics and mass isotopomer analysis as a strategy for pathway discovery: pyrrolyl and cyclopentenyl derivatives of the pro-drug of abuse, levulinate. *Chem. Res. Toxicol.* **26:** 213–220.
6. Zhang, G. F., R. S. Kombu, T. Kasumov, Y. Han, S. Sadhukhan, J. Zhang, L. M. Sayre, D. Ray, K. M. Gibson, V. A. Anderson, et al. 2009. Catabolism of 4-hydroxyacids and 4-hydroxynonenal via 4-hydroxy-4-phosphoacyl-CoAs. *J. Biol. Chem.* **284:** 33521–33534.
7. Zhang, G. F., S. Sadhukhan, G. P. Tochtrop, and H. Brunengraber. 2011. Metabolomics, pathway regulation, and pathway discovery. *J. Biol. Chem.* **286:** 23631–23635.
8. Zhang, G. F., S. Sadhukhan, R. A. Ibarra, S. M. Lauden, C. Y. Chuang, S. Sushailo, P. Chatterjee, V. E. Anderson, G. P. Tochtrop, and H. Brunengraber. 2012. Metabolism of gamma-hydroxybutyrate in perfused rat livers. *Biochem. J.* **444:** 333–341.
9. Armando, J. W., B. A. Boghigian, and B. A. Pfeifer. 2012. LC-MS/MS quantification of short-chain acyl-CoA's in Escherichia coli demonstrates versatile propionyl-CoA synthetase substrate specificity. *Lett. Appl. Microbiol.* **54:** 140–148.
10. Blachnio-Zabielska, A. U., C. Koutsari, and M. D. Jensen. 2011. Measuring long-chain acyl-coenzyme A concentrations and enrichment using liquid chromatography/tandem mass spectrometry with selected reaction monitoring. *Rapid Commun. Mass Spectrom.* **25:** 2223–2230.
11. Gilibili, R. R., M. Kandaswamy, K. Sharma, S. Giri, S. Rajagopal, and R. Mullangi. 2011. Development and validation of a highly sensitive LC-MS/MS method for simultaneous quantitation of acetyl-CoA and malonyl-CoA in animal tissues. *Biomed. Chromatogr.* **25:** 1352–1359.
12. Hayashi, O., and K. Satoh. 2006. Determination of acetyl-CoA and malonyl-CoA in germinating rice seeds using the LC-MS/MS technique. *Biosci. Biotechnol. Biochem.* **70:** 2676–2681.
13. Haynes, C. A., J. C. Allegood, K. Sims, E. W. Wang, M. C. Sullards, and A. H. Merrill, Jr. 2008. Quantitation of fatty acyl-coenzyme As in mammalian cells by liquid chromatography-electrospray ionization tandem mass spectrometry. *J. Lipid Res.* **49:** 1113–1125.
14. Kasuya, F., Y. Oti, T. Tatsuki, and K. Igarashi. 2004. Analysis of medium-chain acyl-coenzyme A esters in mouse tissues by liquid chromatography-electrospray ionization mass spectrometry. *Anal. Biochem.* **325:** 196–205.
15. Mauriala, T., K. H. Herzig, M. Heinonen, J. Idziak, and S. Auriola. 2004. Determination of long-chain fatty acid acyl-coenzyme A compounds using liquid chromatography-electrospray ionization tandem mass spectrometry. *J. Chromatogr. B Analyt. Technol. Biomed. Life Sci.* **808:** 263–268.
16. Minkler, P. E., J. Kerner, T. Kasumov, W. Parland, and C. L. Hoppel. 2006. Quantification of malonyl-coenzyme A in tissue specimens by high-performance liquid chromatography/mass spectrometry. *Anal. Biochem.* **352:** 24–32.
17. Park, J. W., W. S. Jung, S. R. Park, B. C. Park, and Y. J. Yoon. 2007. Analysis of intracellular short organic acid-coenzyme A esters from actinomycetes using liquid chromatography-electrospray ionization-mass spectrometry. *J. Mass Spectrom.* **42:** 1136–1147.
18. Perera, M. A., S. Y. Choi, E. S. Wurtele, and B. J. Nikolau. 2009. Quantitative analysis of short-chain acyl-coenzymeAs in plant tissues by LC-MS-MS electrospray ionization method. *J. Chromatogr. B Analyt. Technol. Biomed. Life Sci.* **877:** 482–488.
19. Sun, D., M. G. Cree, and R. R. Wolfe. 2006. Quantification of the concentration and 13C tracer enrichment of long-chain fatty acyl-coenzyme A in muscle by liquid chromatography/mass spectrometry. *Anal. Biochem.* **349:** 87–95.
20. Magnes, C., M. Suppan, T. R. Pieber, T. Moustafa, M. Trauner, G. Haemmerle, and F. M. Sinner. 2008. Validated comprehensive analytical method for quantification of coenzyme A activated compounds in biological tissues by online solid-phase extraction LC/MS/MS. *Anal. Chem.* **80:** 5736–5742.
21. Minkler, P. E., J. Kerner, S. T. Ingalls, and C. L. Hoppel. 2008. Novel isolation procedure for short-, medium-, and long-chain acyl-coenzyme A esters from tissue. *Anal. Biochem.* **376:** 275–276.
22. Magnes, C., F. M. Sinner, W. Regittnig, and T. R. Pieber. 2005. LC/MS/MS method for quantitative determination of long-chain fatty acyl-CoAs. *Anal. Chem.* **77:** 2889–2894.
23. Dalluge, J. J., S. Gort, R. Hobson, O. Selifonova, F. Amore, and R. Gokarn. 2002. Separation and identification of organic acid-coenzyme A thioesters using liquid chromatography/electrospray ionization-mass spectrometry. *Anal. Bioanal. Chem.* **374:** 835–840.
24. Gu, L., G. F. Zhang, R. S. Kombu, F. Allen, G. Kutz, W. U. Brewer, C. R. Roe, and H. Brunengraber. 2010. Parenteral and enteral metabolism of anaplerotic triheptanoin in normal rats. II. Effects on lipolysis, glucose production, and liver acyl-CoA profile. *Am. J. Physiol. Endocrinol. Metab.* **298:** E362–E371.
25. Suzuki, T., Y. Abiko, and M. Shimizu. 1967. Investigations on pantothenic acid and its related compounds. XII. Biochemical studies (7). Dephospho-coA pyrophosphorylase and dephospho-coA kinase as a possible bifunctional enzyme complex. *J. Biochem.* **62:** 642–649.
26. Peterson, K. L., and D. K. Srivastava. 1997. Functional role of a distal (3′-phosphate) group of CoA in the recombinant human liver

medium-chain acyl-CoA dehydrogenase-catalysed reaction. *Biochem. J.* **325:** 751–760.
27. Wadler, C., and J. E. Cronan. 2007. Dephospho-CoA kinase provides a rapid and sensitive radiochemical assay for coenzyme A and its thioesters. *Anal. Biochem.* **368:** 17–23.
28. Silva, M. F., L. Ijlst, P. Allers, C. Jakobs, M. Duran, I. T. de Almeida, and R. J. Wanders. 2004. Valproyl-dephosphoCoA: a novel metabolite of valproate formed in vitro in rat liver mitochondria. *Drug Metab. Dispos.* **32:** 1304–1310.
29. Huang, K. P. 1970. A sensitive assay method of acetyl CoA synthetase. *Anal. Biochem.* **37:** 98–104.
30. Caraux, G., and S. Pinloche. 2005. PermutMatrix: a graphical environment to arrange gene expression profiles in optimal linear order. *Bioinformatics.* **21:** 1280–1281.
31. Brunengraber, H., and C. R. Roe. 2006. Anaplerotic molecules: current and future. *J. Inherit. Metab. Dis.* **29:** 327–331.
32. Kasumov, T., A. V. Cendrowski, F. David, K. A. Jobbins, V. E. Anderson, and H. Brunengraber. 2007. Mass isotopomer study of anaplerosis from propionate in the perfused rat heart. *Arch. Biochem. Biophys.* **463:** 110–117.
33. Chen, C. T., J. T. Green, S. K. Orr, and R. P. Bazinet. 2008. Regulation of brain polyunsaturated fatty acid uptake and turnover. *Prostaglandins Leukot. Essent. Fatty Acids.* **79:** 85–91.
34. Hamilton, J. A., and K. Brunaldi. 2007. A model for fatty acid transport into the brain. *J. Mol. Neurosci.* **33:** 12–17.
35. Coon, M. J. 2005. Omega oxygenases: nonheme-iron enzymes and P450 cytochromes. *Biochem. Biophys. Res. Commun.* **338:** 378–385.
36. Bazinet, R. P. 2009. Is the brain arachidonic acid cascade a common target of drugs used to manage bipolar disorder? *Biochem. Soc. Trans.* **37:** 1104–1109.
37. Lipton, P. 1999. Ischemic cell death in brain neurons. *Physiol. Rev.* **79:** 1431–1568.